

## Multiple muons in the Utah detector. I. Measurement\*

G. H. Lowe,<sup>†</sup> M. O. Larson, H. E. Bergeson, J. W. Cardon, J. W. Keuffel,<sup>†</sup> and J. West  
*Department of Physics, University of Utah, Salt Lake City, Utah 84112*

(Received 18 February 1975)

Final and more extensive data on multiple-muon events deep underground in the Utah muon detector are presented as rates for multiplicities 1 to 5 in a fiducial plane of 80 m<sup>2</sup>. New results are presented for showers having muon multiplicities from 10 to 50 in a fiducial plane of 100 m<sup>2</sup>. The measurements are taken at depths ranging from a minimum of  $1.5 \times 10^5$  g cm<sup>-2</sup> to a maximum of  $1.0 \times 10^6$  g cm<sup>-2</sup>. The energy per nucleon of the primaries which create the muon shower ranges from  $10^{13}$  to  $10^{16}$  eV.

### I. INTRODUCTION

The advent of the CERN-ISR and Fermilab machines, together with recent theoretical developments of limiting fragmentation and scaling, make it especially interesting now to look for cosmic-ray measurements sensitive to the detailed features of the models of hadronic interactions under consideration. Multiple muons observed deep underground offer special promise in this regard, for they carry rather direct information about the particles produced in the early stages, often from the very first collision, in the hadronic cascade produced by a cosmic-ray primary. Their interpretation is greatly facilitated by the scaling theory, which provides a framework against which the observations may be tested. The framework is anchored by accelerator results near 1 TeV, and scaling provides a clear prescription for extrapolation to cosmic-ray energies. Deviations from the scaling prediction, should there be any, may then be interpreted in terms of the onset of some new phenomena.

However, the predictions depend not only on the collision model, but also on the spectrum and composition assumed for the primaries. The degree to which the spectrum effects can be separated out from the effects of the collision model is not yet fully known, although the richness of the multiple muon data, together with the availability of information from other sources about the spectrum, indicates that some separation can be carried out.

In this paper, we describe the techniques whereby the multiple muons are studied with the Utah cosmic-ray detector and summarize results obtained with expanded 80-m<sup>2</sup> and 100-m<sup>2</sup> fiducial planes. Earlier work<sup>1</sup> has been limited to a restricted area of the detector much smaller for the most part. Comparisons with scaling predictions are given in paper II along with implications of the results for the spectrum and composition of the primaries.

### II. INFORMATION CARRIED BY MULTIPLE MUONS UNDERGROUND

In order to see how muons observed deep underground may be used to study the properties of hadronic collisions high in the atmosphere, it is useful to consider the schematic diagram shown in Fig. 1. A primary (say a proton of  $10^{15}$  eV) strikes the top of the atmosphere and initiates a hadronic cascade. Pions (and kaons) in the cascade may decay to produce muons, the average decay probability for high-energy pions produced by nucleons being  $P_D \approx (90 \text{ GeV}/E_\pi) \sec\theta$ . The rock above the Utah detector acts as a muon range analyzer; by looking in different directions, muon energy thresholds from 0.5 to 20 TeV may be imposed.

The quantities actually observed are (a) the rates  $J(n_D, \theta, h)$  of events where  $n_D$  muons traverse the 80 m<sup>2</sup> or 100 m<sup>2</sup> fiducial area of the detector at a slant depth  $h$  and a zenith angle  $\theta$ , and (b) the lateral separation distribution of the muons. A later paper will give further results on the separation of the muons.

Ideally, one would like to extract from the observed quantities information about the basic parameters of the collision model: the total cross section, the multiplicity, the distribution in longitudinal momentum of the produced particles, and the transverse momentum, all as a function of the primary energy. The muons observed come, of course, from a random sample of the produced pions and kaons, and it is necessary to investigate with the aid of a Monte Carlo calculation the degree to which this sample is sensitive to the assumed hadronic collision model.

### III. APPARATUS

The detector has been described in some detail.<sup>2-5</sup> Briefly, it consists of 600 cylindrical spark counters arrayed in 15 vertical planes, each  $6 \times 10$  m<sup>2</sup> as shown in Figs. 2 and 3. A trig-

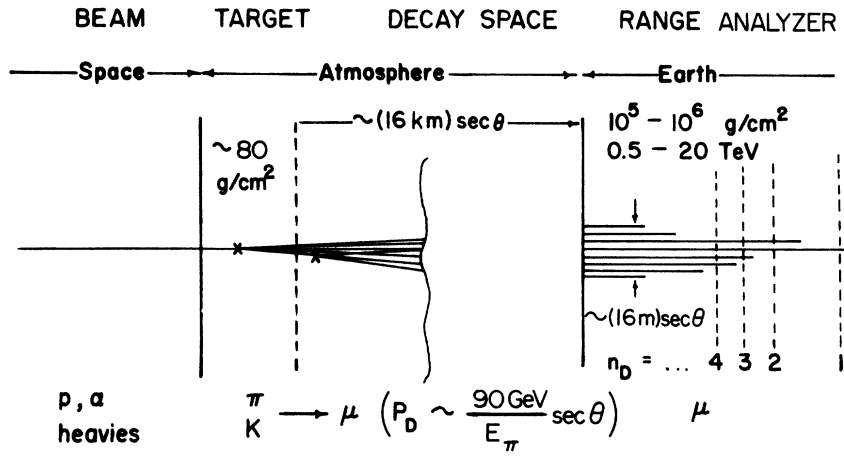
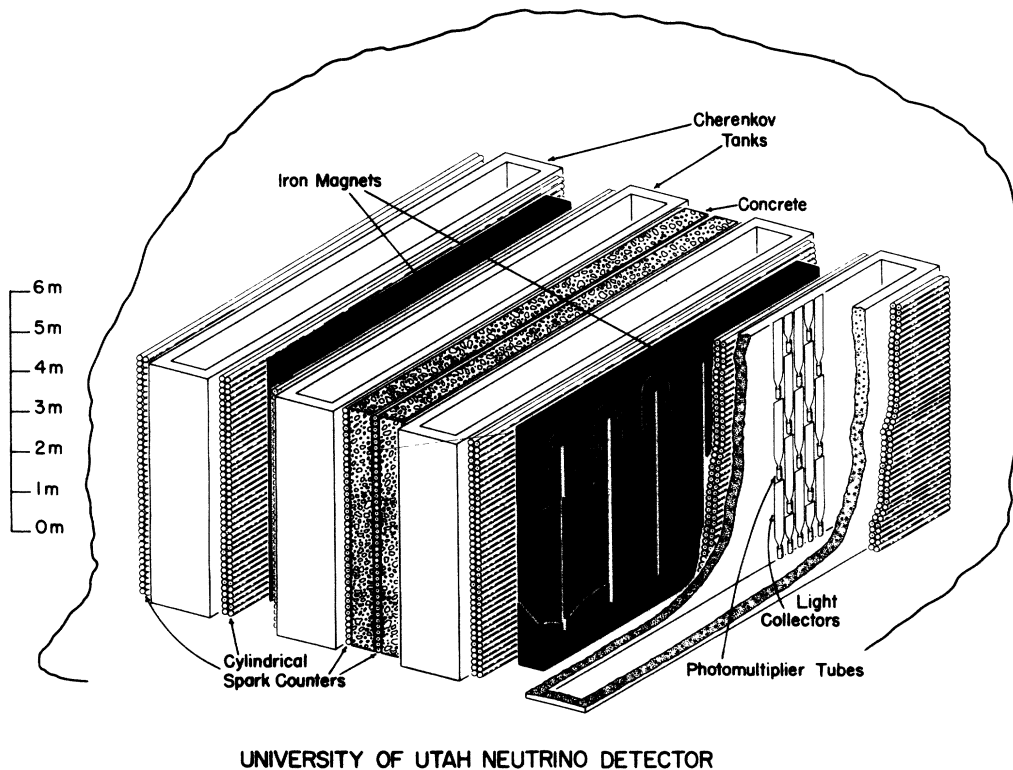


FIG. 1. Schematic diagram of the high-energy muon component of an energetic cosmic-ray event.

ger is provided by water-filled Cherenkov counters. The spark counters resemble oversized Geiger counters, 15 cm dia.  $\times$  10 m long, but operated in a pulsed mode at a higher pressure

so that the discharge is a sharply localized corona spike which is detected by means of a sonic ranging system. The location along the axis of the spark counter is known to within  $\pm$  3 mm.



UNIVERSITY OF UTAH NEUTRINO DETECTOR

FIG. 2. The Utah neutrino detector. The detector is 12 m by 10 m by 6 m. Its mass is  $1.8 \times 10^6$  kg. The three major components of the detector are (1) four directional Cherenkov tanks indicating the passage of a right- or left-going muon, (2) 15 stacks of 40 sonic ranging cylindrical spark counters which provide muon trajectory information, and (3) two iron magnets which determine the charge of the muon.

Originally the detector had a ferrite core memory capable of storing information from as many as 108 sparks in the cylindrical spark counters for any given event. Since, on the average, each muon in the detector has associated with it 10 sparks, the ferrite core memory severely limited the maximum observable multiplicity. In early 1973 the ferrite core memory was replaced with

a semiconductor shift register memory capable of storing information from 1000 sparks. These data were recorded on magnetic tapes, which provide the basis for computer reconstruction and analysis of muon showers in the detector.

The data analysis is divided into two sections which overlap somewhat:

(I) Rates for  $J(n_D)$  in  $80 \text{ m}^2$ ,  $n_D < 10$  with zenith

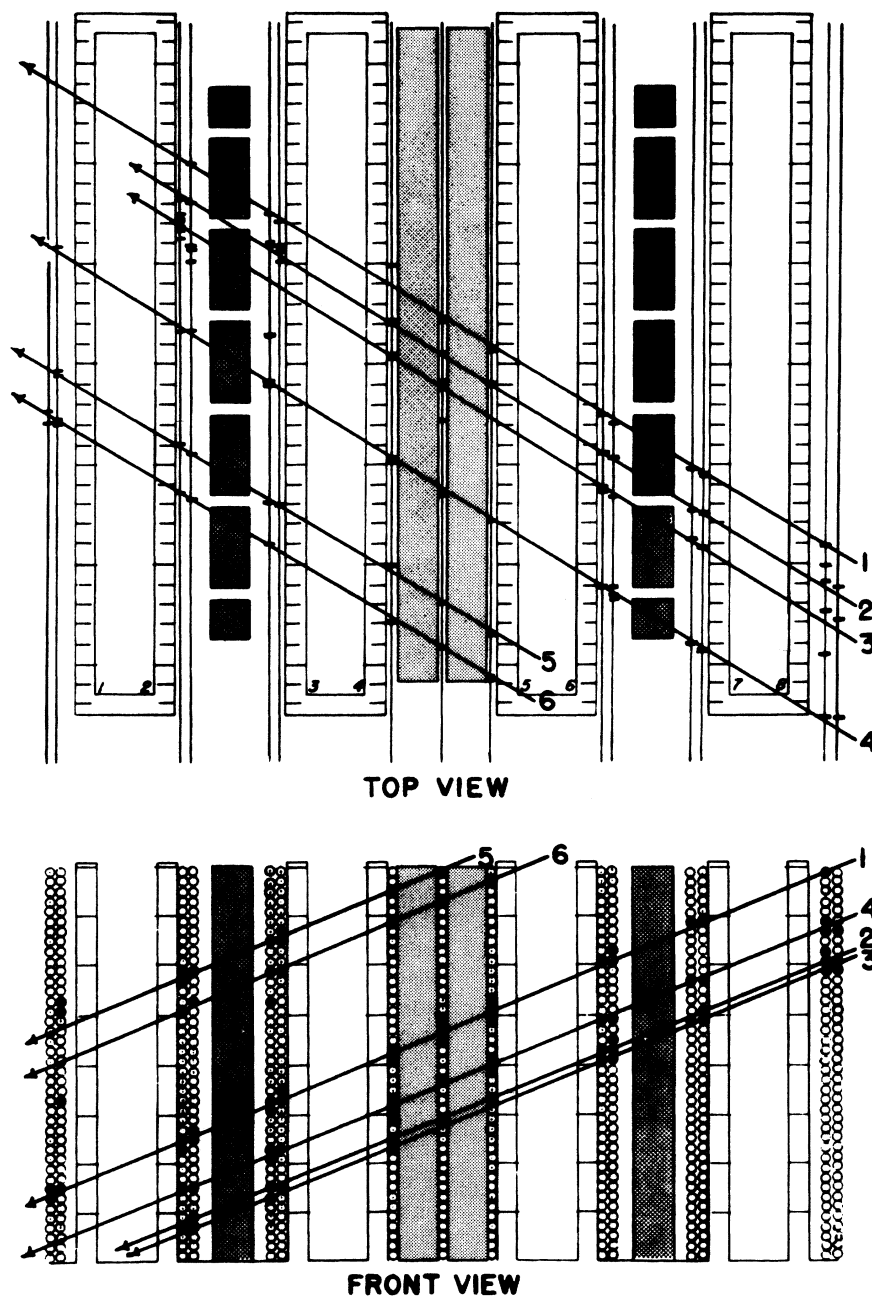


FIG. 3. Plot of an event containing six muons. The coordinates of the sparks in the top view are obtained from the time delays of the acoustical pulses.

angles greater than  $35^\circ$  and less than 108 sparks in an event (low multiplicity). The data were taken in three blocks with run times of  $1.81 \times 10^7$  sec,  $2.523 \times 10^7$  sec, and  $1.855 \times 10^7$  sec from February 1969 to June 1974. Other than the statistical treatment of bins with a low number of counts,<sup>6</sup> details of the analysis are available elsewhere.<sup>7</sup>

(II) Rates for  $J(n_D)$  in  $100 \text{ m}^2$ ,  $n_D \geq 10$  with an average zenith angle of  $30^\circ$  (high multiplicity). The data were taken with the new enlarged memory over a period from May 1973 to June 1974 with  $2.031 \times 10^7$  sec live time. Details of the analysis can be found in the Appendix. Description of Analysis I (low-multiplicity events) follows below, and description of Analysis II (high-multiplicity events) begins in Sec. V.

#### IV. ANALYSIS I (LOW-MULTIPLICITY EVENTS)

A pattern-recognition computer program is used for event detection. The efficiency of the recognition program was measured and found to range from greater than 99% for events which contain one muon in the detector to  $96 \pm 5\%$  for events which contain five muons in the detector. Efficiency of the recognition program drops off considerably for muon trajectories separated by 0.25 meters or less. At least 100 events of every muon multiplicity were hand-scanned and in total more than 6000 events were hand-scanned to check event recognition efficiency. The angle between muon tracks within the detector was on the average less than 1 degree and no evidence of convergence or divergence of the tracks was found.

The actual area of the detector perpendicular to muons which pass through three or more groups of spark counters varies considerably in both size and shape as the zenith and azimuth angles of incoming muons are varied. However, the Cherenkov triggering walls of the detector, when projected into a plane perpendicular to the direction of travel of the muons in an event, form a figure which is fairly constant in area and shape. The mean area of this figure is somewhat greater than  $80 \text{ m}^2$  at zenith angles greater than  $30^\circ$ .

All muons in an event are required to pass through an imaginary plane of  $80 \text{ m}^2$  independent of angle which is superimposed on the detector. If this "superplane" were sensitive over its entire area, the acceptance criteria for all events would be the same for the same zenith angle bin. However, there are insensitive holes in the superplane for which corrections to the above simple aperture must be made. With muons which pass through only two groups of spark counters accepted in the analysis (the pattern-recognition program

picks up greater than 90% of the two-group muons which are parallel to a three-group muon) only small parts of the imaginary  $80\text{-m}^2$  plane are insensitive to a through-going muon.

The corrections to the aperture are made assuming muons in events on the average are distributed uniformly over the detector. Earlier measurements<sup>1</sup> have shown that the rate of pairs in two  $1\text{-m}^2$  detectors distance  $x$  apart (the "decoherence curve") can be characterized approximately by the form  $Ae^{-x/x_0}$ , where  $x_0 \approx 10 \text{ m}$  at  $\theta = 45^\circ$ , depth =  $2.4 \times 10^5 \text{ g cm}^{-2}$ . The rate of inclusive doubles (inclusive here used in the same manner as in accelerator experiments) is given by

$$R(2\text{'s inclusive}) = \sum_{n_D > 1} \frac{n_D! J(n_D)}{2!(n_D - 2)!} \\ = \iint_{\text{area of detector}} \frac{A}{2} \exp(-x/x_0) dA_1 dA_2, \quad (1)$$

where  $x$  is the distance between the two small detectors  $dA_1$  and  $dA_2$ . Calculations were made of the integral using measured values of the decoherence curve. With a value of  $x_0$  of 10 m, changing the shape of the detector from  $\sqrt{80} \text{ m} \times \sqrt{80} \text{ m}$  to  $5 \times 16 \text{ m}$  changes the rate of inclusive doubles by 8%. Thus, one expects the assumption of uniform distribution to be accurate for the much smaller changes in detector shape in the experiment.

The rates were tested as a function of the size of the correction factor applied to the data. No discernible effect was disclosed. However, only data where the correction to the aperture was small were used in the final analysis.

The triggering efficiency of the detector was measured in the following manner. For Cherenkov tanks, a muon was required to pass within prescribed boundaries on the inside of the tank and an independent trigger associated with a muon must have been produced by tanks other than the one being measured. Spark-counter efficiencies were measured by requiring that a trajectory be recognizable without the presence of the counter being measured. Extensive tests were made of the consistencies of the triggering logic.

The rates were corrected for the measured detector triggering efficiency. As the number of muons passing through the detector in an event increases, the average amount of light in each Cherenkov tank increases and the triggering efficiency of the detector approaches 100%. With the new Cherenkov triggering system installed in 1970, the average single-muon event triggering

efficiency was 90% (see Ref. 3) at the beginning of 1971 and deteriorated to 83% by 1974. The average double-muon event efficiency was 91% and showed no change with time. Single spark-counter efficiency averaged 90%. With the redundancy of spark counters, less than 4% of the single muons and fewer multiples were lost.

The first block of data (1969) was not used for single muon rates due to relatively low Cherenkov efficiencies. Rates for muon multiplicities greater than one showed no systematic change between the three data blocks.

Rock depths for different  $\theta$  (zenith) -  $\phi$  (azimuth) bins were determined from 7.5 minute series topographical maps of the U. S. Geological Survey to an accuracy of 6 m.<sup>8</sup> These depths were converted into grams per square centimeter by multiplying by the rock density. Direct measurements of the density are limited in the number of points of access where samples may be taken, but an average of 2.61 was adopted by Keuffel *et al.*<sup>9</sup> Cassidy *et al.*<sup>10</sup> measured the vertical muon intensity at 10 locations along the access tunnel to the detector, and by comparison with the world survey curve deduced a density of  $2.55 \pm 0.04$ . The Cassidy measurements surveyed the rock which corresponds to a slant depth around  $2.4 \times 10^5$  g cm<sup>-2</sup> for the detector. In order that the muon-flux data fit a survey of the world depth-intensity curve,<sup>11,12</sup> it was assumed that for depths less than  $2.8 \times 10^5$  g cm<sup>-2</sup> the density was 2.55 and for greater depths the density was 2.59. A  $Z^2/A$  correction has been made in order to convert the Utah rock which has a  $Z^2/A$  of 5.65 to standard rock which has a  $Z^2/A$  of 5.50.<sup>13</sup> Atmospheric depth traversed has been added on to the rock depth in grams per square centimeter to give total depth.

Since the data are scattered over a wide range of depths and zenith angles, it is necessary to consolidate them in some way. The first step in this procedure is to study the depth dependence of the rates. Rates at fixed  $\theta$  and  $n_D$  were fitted as a function of depth using the method of maximum likelihood. A Gaussian probability distribution was used<sup>7</sup> where the number of counts are large ( $\sim 40$ /bin) and a Poisson<sup>6</sup> when the number of counts are small. This function of depth was then used to center the data in  $8 \times 10^4$ -g cm<sup>-2</sup> bins and  $5^\circ$   $\theta$  bins. Systematic errors due to rock-density fluctuations, rather than statistical error, dominate in depth-angle ranges where the number of counts is high. Each depth-angle range has a number of contributions from different azimuthal angles. The most likely value of the rate for each depth-angle range was found, and the errors for the bin were multiplied by root reduced  $\chi^2$  for reduced  $\chi^2$  greater than one.

Rates for the presented data were consistent within the three blocks of data. Rates for multiplicities in the range  $5 < n_D < 10$  were found to have significant contributions from events which had greater than 108 sparks. Analysis of these data is underway. The rates for  $n_D = 5$  at  $2.4 \times 10^5$  g cm<sup>-2</sup> are corrected for the small contribution from events having greater than 108 sparks.

Table I summarizes the data. The indicated errors are Gaussian and take into account depth centering errors. Figure 4 shows sample depth dependences and relative intensities at angles used for the Monte Carlo analysis in paper II. The similarity of the depth dependences for all multiplicities is immediately obvious. Note that the muon flux (intensity of inclusive singles) is given by

$$I(\text{inclusive singles}) = \sum_{n_D} n_D J(n_D) / 80 \text{ m}^2. \quad (2)$$

However, the contribution from multiples greater than one is small since the rate of doubles in 80 m<sup>2</sup> is one to two percent of that of singles.

#### V. ANALYSIS II (HIGH-MULTIPLICITY EVENTS)

The pattern recognition program discussed in Sec. IV proved to be inefficient and inaccurate in analyzing events with more than 100 sparks in the counters. These events tended to have muons at small zenith angles. A new analysis scheme was developed to handle these more complex events using a program which worked on groups of sparks instead of individual sparks. Details are given in the Appendix. Muons which were closer together than 0.29 m were considered to be one muon for purposes of the analysis.

Events which proved too difficult for the program were hand-scanned. The scanning showed the average muon count to be good to within 10%.

At zenith angles less than  $45^\circ$  the detector has over 100 m<sup>2</sup> of sensitive area. The actual counting area was limited to 100 m<sup>2</sup> since the muon detector efficiency falls off near the edge of the detector.

Detector triggering efficiency was greater than 99% with dead time excluded. Spark counter efficiency corrections were negligible due to the large counter redundancy at small zenith angles.

A total of  $6 \times 10^2$  events were observed. These events were binned at a mean zenith angle of  $30^\circ$  in the depth ranges  $(1.4-1.8) \times 10^5$  g cm<sup>-2</sup>,  $(1.8-2.2) \times 10^5$  g cm<sup>-2</sup>,  $(2.2-3.0) \times 10^5$  g cm<sup>-2</sup>,  $(3.0-3.8) \times 10^5$  g cm<sup>-2</sup> and multiplicity ranges 10-14, 15-19, 20-29, 30-49, and  $\geq 50$ .

The data were centered by the same means as analysis I except that only Poisson statistics

TABLE I. Rates in 80-m<sup>2</sup> detector (sec<sup>-1</sup>sr<sup>-1</sup>).

Depth (10 <sup>5</sup> g cm <sup>-2</sup> )	Zenith angle (deg)	$n_D=1$	$n_D=2$	$n_D=3$	$n_D=4$	$n_D=5$
		$(7.86 \pm 0.40) \times 10^{-2}$	$(1.58 \pm 0.10) \times 10^{-3}$	$(1.82 \pm 0.14) \times 10^{-4}$	$(5.9 \pm 0.9) \times 10^{-5}$	$(2.5 \pm 0.7) \times 10^{-5}$
	47.5	$(8.44 \pm 0.53) \times 10^{-2}$	$(1.55 \pm 0.11) \times 10^{-3}$	$(1.84 \pm 0.17) \times 10^{-4}$	$(5.2 \pm 1.3) \times 10^{-5}$	$(2.6 \pm 0.7) \times 10^{-5}$
3.2	47.5	$(2.14 \pm 0.15) \times 10^{-2}$	$(3.98 \pm 0.34) \times 10^{-4}$	$(4.4 \pm 0.8) \times 10^{-5}$	$(1.6 \pm 0.4) \times 10^{-5}$	$(4.0 \pm 2.0) \times 10^{-6}$
	52.5	$(2.39 \pm 0.18) \times 10^{-2}$	$(4.29 \pm 0.38) \times 10^{-4}$	$(5.3 \pm 0.6) \times 10^{-5}$	$(1.9 \pm 0.3) \times 10^{-5}$	$(5.9 \pm 1.1) \times 10^{-6}$
	57.5	$(2.76 \pm 0.20) \times 10^{-2}$	$(4.49 \pm 0.37) \times 10^{-4}$	$(5.2 \pm 0.5) \times 10^{-5}$	$(1.31 \pm 0.16) \times 10^{-5}$	$(4.3 \pm 0.9) \times 10^{-6}$
	62.5	$(3.13 \pm 0.22) \times 10^{-2}$	$(4.25 \pm 0.33) \times 10^{-4}$	$(4.24 \pm 0.48) \times 10^{-5}$	$(1.6 \pm 0.5) \times 10^{-5}$	$(2.8 \pm 1.1) \times 10^{-6}$
4.0	62.5	$(9.12 \pm 0.80) \times 10^{-3}$	$(1.38 \pm 0.12) \times 10^{-4}$	$(1.7 \pm 0.2) \times 10^{-5}$	$(3.5 \pm 0.9) \times 10^{-6}$	$(1.3 \pm 0.6) \times 10^{-6}$
	67.5	$(1.11 \pm 0.09) \times 10^{-2}$	$(1.34 \pm 0.14) \times 10^{-4}$	$(1.38 \pm 0.30) \times 10^{-5}$	$(3.2 \pm 2.1) \times 10^{-6}$	$(0.93 \pm 0.44) \times 10^{-6}$
	72.5	$(1.46 \pm 0.11) \times 10^{-2}$	$(1.34 \pm 0.24) \times 10^{-4}$	$(1.28 \pm 0.40) \times 10^{-5}$	$(0.78 \pm 0.97) \times 10^{-6}$	
4.8	62.5	$(3.31 \pm 0.70) \times 10^{-3}$	$(5.52 \pm 0.80) \times 10^{-5}$	$(5.3 \pm 1.9) \times 10^{-6}$		
	67.5	$(4.41 \pm 0.42) \times 10^{-3}$	$(5.58 \pm 0.62) \times 10^{-5}$	$(5.2 \pm 1.2) \times 10^{-6}$	$(0.43 \pm 0.35) \times 10^{-6}$	$(0.49 \pm 0.35) \times 10^{-6}$
	72.5	$(4.65 \pm 0.44) \times 10^{-3}$	$(5.2 \pm 0.6) \times 10^{-5}$	$(3.4 \pm 0.9) \times 10^{-6}$	$(1.4 \pm 0.6) \times 10^{-6}$	
5.6	67.5	$(1.39 \pm 0.16) \times 10^{-3}$	$(1.5 \pm 0.4) \times 10^{-5}$	$(2.0 \pm 0.9) \times 10^{-6}$		
	72.5	$(1.90 \pm 0.22) \times 10^{-3}$	$(2.0 \pm 0.4) \times 10^{-5}$	$(1.5 \pm 0.6) \times 10^{-6}$	$(0.17 \pm 0.24) \times 10^{-6}$	
	77.5	$(2.42 \pm 0.26) \times 10^{-3}$	$(0.99 \pm 0.19) \times 10^{-5}$	$(0.75 \pm 0.46) \times 10^{-6}$		
6.4	72.5	$(7.7 \pm 1.2) \times 10^{-4}$	$(1.2 \pm 0.3) \times 10^{-5}$	$(1.8 \pm 1.0) \times 10^{-6}$	$(0.5 \pm 0.6) \times 10^{-6}$	
	77.5	$(8.8 \pm 1.1) \times 10^{-4}$	$(0.37 \pm 0.12) \times 10^{-5}$	$(0.23 \pm 0.28) \times 10^{-6}$		
7.2	72.5	$(3.3 \pm 0.5) \times 10^{-4}$	$(0.35 \pm 0.13) \times 10^{-5}$	$(0.42 \pm 0.50) \times 10^{-6}$		
	77.5	$(3.5 \pm 0.5) \times 10^{-4}$	$(0.25 \pm 0.11) \times 10^{-5}$			
8.0	77.5	$(1.34 \pm 0.25) \times 10^{-4}$	$(0.15 \pm 0.07) \times 10^{-5}$			
	82.5	$(2.0 \pm 0.3) \times 10^{-4}$				

could be used because of the low numbers of counts in individual bins. No obvious zenith angle dependence could be discerned, so a mean zenith angle of 30° was used and events at all angles were combined for events in the depth range 1.4–2.2  $\times 10^5$  g cm<sup>-2</sup>. Mean zenith angles are indicated for greater depths. Table II summarizes the data. The indicated errors include depth centering errors and are Gaussian.

## VI. DISCUSSION

These results have been shown<sup>7</sup> to be consistent with earlier measurements<sup>1</sup> made at Utah. They are, however, considerably more extensive, have a larger detector area, and are not dependent upon model calculations. Comparison of the earlier results at Utah with a model of the shower interactions can be found in papers by the Durham cos-

mic-ray group.<sup>14</sup> Other multiple muon measurements and analysis of them have been made by a group from the University of Tokyo.<sup>15</sup> Their experiment was carried out at an average depth of  $1.38 \times 10^5$  g cm<sup>-2</sup> with a detector area of 8.4 m<sup>2</sup>. The highest observed muon multiplicity was 18.

The size of the Utah detector might be called intermediate compared to the size of a typical shower. The rate of events with multiplicity  $n_D$  should be proportional to the area of the detector to the power  $n_D$  in a small detector and proportional to the area in a large detector. In work done at Utah<sup>7</sup> the ratio of inclusive doubles in 80 m<sup>2</sup> to inclusive doubles in 20 m<sup>2</sup> was shown to be about 13 at a zenith angle of 47.5° and a depth of  $2.4 \times 10^5$  g cm<sup>-2</sup>. With both areas small (large) compared to the size of a shower this ratio would be 16 (4). The observation of decoherence curve exponential falloff lengths  $x_0$  around 10 m also indicates that the

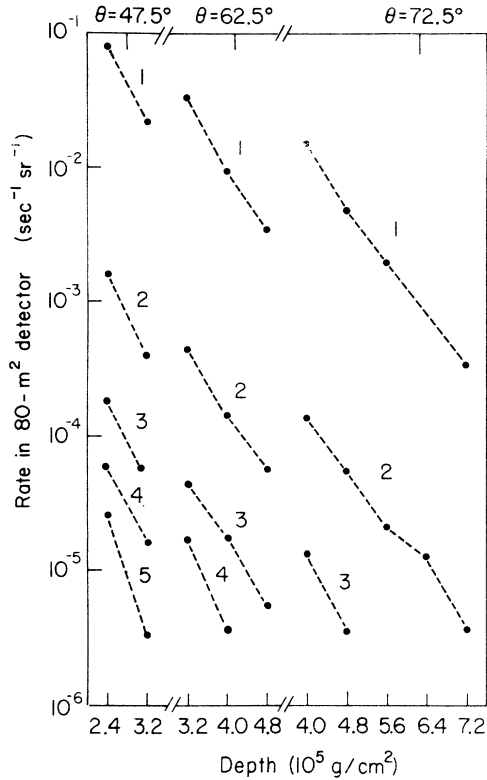


FIG. 4. Rates of multiplicities 1–5 as a function of depth at three different zenith angles.

detector is intermediate in size.

Consideration of the intermediate size of the detector leads to an understanding of the relatively flat zenith angle dependence of the rates of events with muon multiplicity greater than one. Muons in more steeply inclined events have an increased lateral spread since they are produced at greater distances, and this compensates for the higher decay probability of their parents due to the thinner atmosphere. The angular depen-

dence of the muon flux (inclusive singles) is in agreement with a  $\sec\theta$  enhancement, which is based upon pion and kaon parentage of the muons.<sup>12</sup>

Although the muon flux is dependent upon the intensity of primaries at a given energy per nucleon, multiple-muon events are more dependent upon the intensity of primaries at a given total energy or energy per nucleus. A rough estimate of the primary energies which generate muon showers can easily be made relating the energy of the muons to the primary energy by taking into account detector size and decay probabilities. This yields about  $2 \times 10^{15}$  eV for the primary energy of a 30-muon event at a depth of  $1.6 \times 10^5$  g cm<sup>-2</sup>. The Monte Carlo calculation in paper II gives  $6 \times 10^{15}$  eV for the median energy of the incident protons which would create the 30-muon event. Since the range of energies which contribute to high-multiplicity events is quite large, a significant fraction of the detected events come from energies above  $10^{16}$  eV. These measurements offer a unique chance for a preliminary peek at the properties of the initial hadronic interaction at energies considerably above the energies of present accelerators (up to a factor of  $10^4$ ). The Monte Carlo calculations in paper II indicate that Feynman scaling and simple assumptions about the cosmic-ray spectrum provide reasonably good agreement with these multiple-muon results.

#### ACKNOWLEDGMENTS

The authors are grateful to the many members of the University of Utah Cosmic Ray Group, whose united efforts have made this research possible. We express our gratitude to Al Larsen for his work on the expanded semiconductor shift register memory, to Dave Steck for preparing the computer tapes for our analysis, to Lee Gallegos for event scanning, to V. D. Sandberg for his work on the aperture calculation, and to S. Ozaki for many of the initial concepts. We appreciate many useful discussions with J. L. Morrison.

TABLE II. Rates in 100-m<sup>2</sup> detector (sec<sup>-1</sup> sr<sup>-1</sup>).

Depth (10 <sup>5</sup> g cm <sup>-2</sup> )	Average zenith angle (deg)	$n_D = 10-14$	$n_D = 15-19$	$n_D = 20-29$	$n_D = 30-49$	$n_D \geq 50$
1.6	30	$(4.56 \pm 0.36) \times 10^{-5}$	$(1.47 \pm 0.19) \times 10^{-5}$	$(6.0 \pm 1.3) \times 10^{-6}$	$(1.4 \pm 0.7) \times 10^{-6}$	$(8.0 \pm 5.0) \times 10^{-7}$
2.0	35	$(1.77 \pm 0.20) \times 10^{-5}$	$(5.0 \pm 1.1) \times 10^{-6}$	$(1.9 \pm 0.7) \times 10^{-6}$	$(8.0 \pm 4.0) \times 10^{-7}$	
2.6	50	$(4.5 \pm 0.6) \times 10^{-6}$	$(1.5 \pm 0.3) \times 10^{-6}$	$(7.0 \pm 3.0) \times 10^{-7}$		
3.4	60	$(7.0 \pm 3.0) \times 10^{-6}$	$(4.0 \pm 2.0) \times 10^{-7}$			

We would like to express our deep appreciation to the late Jack Keuffel, who initiated and directed the construction, operation, and data analysis of the Utah muon detector.

#### APPENDIX: ANALYSIS OF HIGH-MULTIPLICITY EVENTS

The Utah detector was optimized for the study of low-multiplicity muon events with roughly horizontal trajectories. However, it turns out to be effective for high-multiplicity events ( $\geq 10$  muons) with zenith angles between  $22^\circ$  and  $45^\circ$ . If one also requires an azimuth angle of less than  $55^\circ$  as measured from a normal to a detector plane, then one can always find a  $100 \text{ m}^2$  area normal to the trajectory (the "impact plane") in which one has near 100% efficiency for muon detection. The minimum zenith angle and the maximum azimuth angle requirements guarantee that each trajectory within the fiducial  $100 \text{ m}^2$  will pass through at least two cylindrical spark counters (CSC) groups with enough absorber between them to reject electrons. Those passing through only two spark-counter groups will be steep enough to penetrate several counters in each group, thus producing enough sparks for trajectory reconstruction. It is virtually certain that different muons will satisfy the triggering requirements of a coincidence between corresponding walls of two Cherenkov tanks.

The high-multiplicity computer program worked on groups of sparks, instead of individual sparks as was the case in the low-multiplicity pattern-recognition program. Two parallel muon trajectories are found by doing least-squares fits to these spark groups in the top, front, and side views. These two parallel trajectories were then assumed to define the direction of all muons in the event and a projection was made into the impact plane. Once in the impact plane the spark projections for a given muon cluster together in a tight group. The computer then searched for these groups. To qualify as a muon there must be at least three sparks which lie within a  $7.5 \text{ cm} \times 12 \text{ cm}$  box in the impact plane. The exact dimensions of the box vary slightly with direction of the muons with respect to the detector and are asymmetrical because of the greater precision in the determination of the spark position along the length of the spark counter. In addition, if the projected trajectory passes through more than two CSC columns it is required that there be sparks within the box in at least 50% of the columns traversed. Furthermore, sparks are required in at least two groups, except in cases where the muon passed through columns 5, 6, and 7, or 9, 10, and 11. In this manner the computer

counts the number of muons in the event.

Since muons frequently have soft accompaniment it is possible for the program to falsely identify 2-3 muons in close proximity. From a visual scan it was found that as the separation between two muons became less than 29 cm there was an increasing probability that one of them was not a muon but rather electron accompaniment. To avoid having several knock-on electrons falsely simulate a muon, tracks closer together than 29 cm were consolidated and considered as a single muon. Beyond this distance it is very unlikely that knock-ons will cluster in the impact plane well enough to meet the criteria imposed. A similar criterion was applied for the theoretical Monte Carlo calculation (for events with multiplicity of 10 or more only) presented in paper II.

The question of whether a single accompanying electron could simulate a muon at separation greater than 29 cm was considered. In order to simulate a muon an electron must traverse at least five CSC walls in order to produce the minimum three sparks needed for each muon. This represents 0.6 radiation length and the electron must be more energetic than 10 MeV. It cannot deviate by more than  $10^\circ$  from the track of the original muon or it will be rejected. Since its projected trajectory almost always takes it through other CSC groups it must produce at least one spark in another group, which is separated from the first by concrete, iron, or water absorber. Electrons produced by muons in the detector will have a negligibly small probability of getting 29 cm away from the producing muon to simulate a muon. It is possible for knock-ons produced in the ceiling to satisfy the separation criterion. It was calculated that 3.7% of the muons have knock-ons associated with them of greater than 10 MeV. However, because of the short radiation length, to simulate a muon these electrons must strike the CSC directly without passing through concrete, water, or steel. In addition, if the electron strikes in the main portion of the detector its projected trajectory will carry it through additional spark counters separated from its entry point by more than 10 radiation lengths. It is nearly impossible for such electrons to produce the additional required sparks. These restrictions leave less than 20% of the area of the  $100 \text{ m}^2$  in which the electron could simulate a muon. Thus, less than 1% of the muons striking the detector will have associated knock-on electrons successfully masquerading as muons. These calculations coupled with meticulous scanning of plots indicate that the individual counts are good to about 10%. Average numbers should be considerably better.



\*Research supported by the National Science Foundation.

‡Present address: ESL Inc., Sunnydale, Calif. 94086.

†Deceased.

<sup>1</sup>K. H. Davis *et al.*, Phys. Rev. D 4, 607 (1971).

<sup>2</sup>H. E. Bergeson and C. J. Wolfson, Nucl. Instrum. Methods 51, 47 (1967).

<sup>3</sup>G. L. Cassiday, D. E. Groom, and M. O. Larson, Nucl. Instrum. Methods 107, 509 (1973).

<sup>4</sup>L. K. Hilton and R. O. Stenerson, Nucl. Instrum. Methods 51, 47 (1967).

<sup>5</sup>J. W. Keuffel and J. L. Parker, Nucl. Instrum. Methods 51, 29 (1967).

<sup>6</sup>G. H. Lowe, Univ. of Utah Internal Report No. UUCR 138, 1974 (unpublished).

<sup>7</sup>G. H. Lowe, Ph.D. thesis, University of Utah, 1972 (unpublished).

<sup>8</sup>G. W. Mason, Ph.D. thesis, University of Utah, 1969

(unpublished); M. O. Larson, Ph.D. thesis, University of Utah, 1968 (unpublished).

<sup>9</sup>J. W. Keuffel *et al.*, Acta Phys. Acad. Sci. Hung. 29, Suppl. 4, 183 (1969).

<sup>10</sup>G. L. Cassiday *et al.*, Phys. Rev. Lett. 27, 164 (1971).

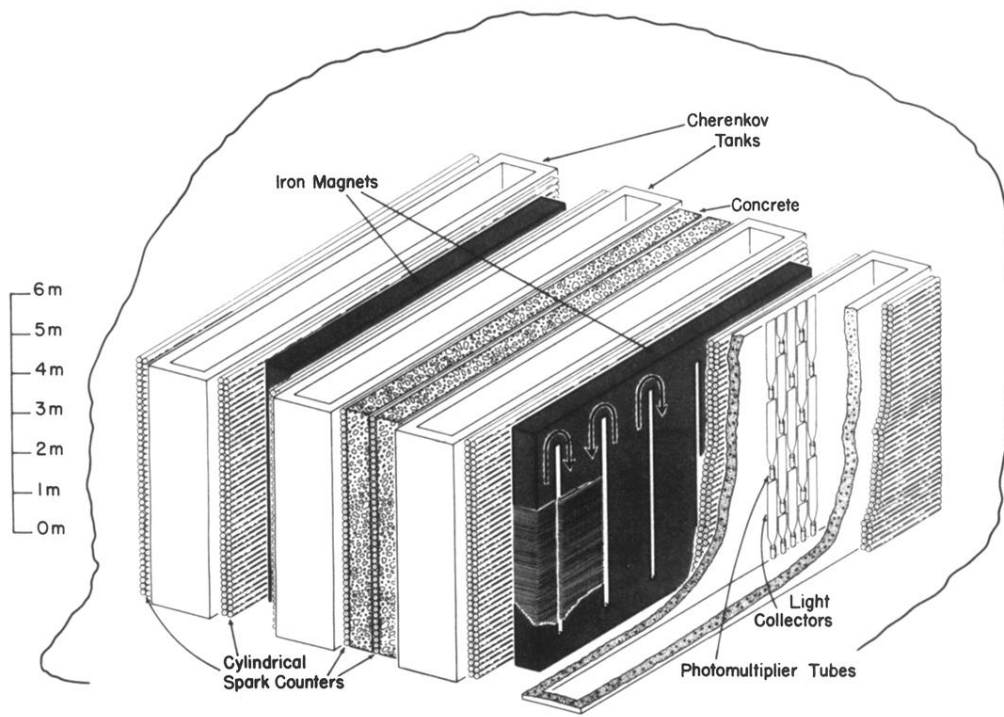
<sup>11</sup>G. W. Carlson, Ph.D. thesis, University of Utah, 1972 (unpublished).

<sup>12</sup>H. E. Bergeson *et al.*, in *Proceedings of the Thirteenth International Conference on Cosmic Rays, 1973* (Colorado Associated Univ. Press, Boulder, 1973), Vol. 3, p. 1722.

<sup>13</sup>E. R. Martin, Ph.D. thesis, University of Utah, 1968 (unpublished).

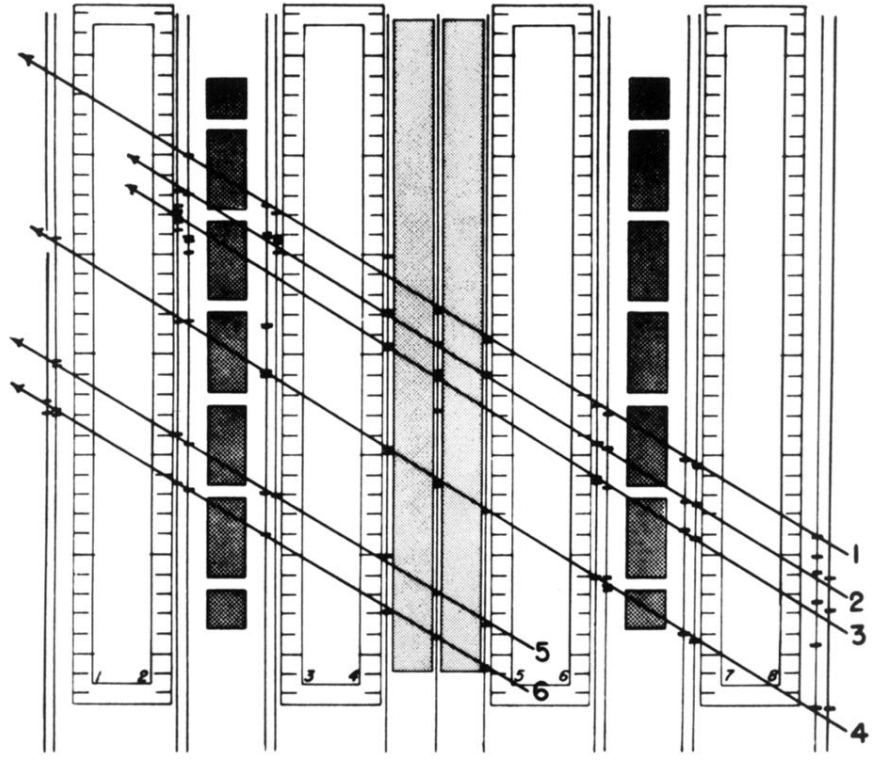
<sup>14</sup>C. Adcock *et al.*, J. Phys. A 2, 354 (1969).

<sup>15</sup>T. Suda, Y. Yotsuka, and M. Koshiba, J. Phys. Soc. Jpn. 36, 351 (1974).

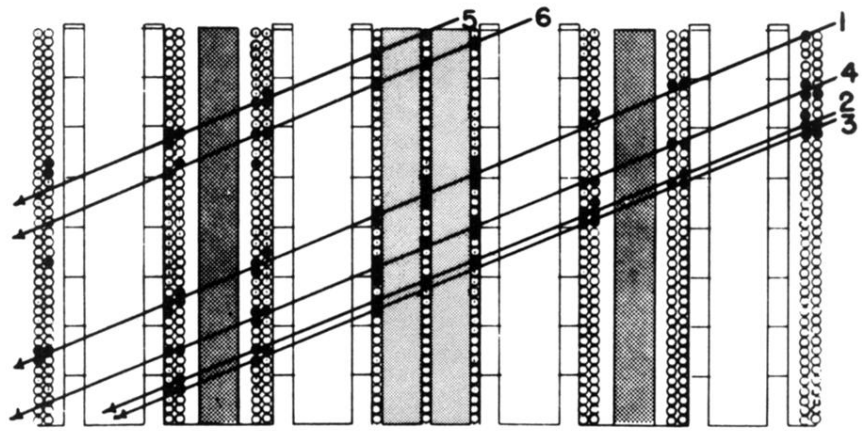


UNIVERSITY OF UTAH NEUTRINO DETECTOR

FIG. 2. The Utah neutrino detector. The detector is 12 m by 10 m by 6 m. Its mass is  $1.8 \times 10^6$  kg. The three major components of the detector are (1) four directional Cherenkov tanks indicating the passage of a right- or left-going muon, (2) 15 stacks of 40 sonic ranging cylindrical spark counters which provide muon trajectory information, and (3) two iron magnets which determine the charge of the muon.



TOP VIEW



FRONT VIEW

FIG. 3. Plot of an event containing six muons. The coordinates of the sparks in the top view are obtained from the time delays of the acoustical pulses.